

## The Nuclear Impact on Cosmology: The $H_0$ - $\Omega$ Diagram

The  $H_0$ - $\Omega$  diagram is resurrected to dramatically illustrate the nature of the key problems in physical cosmology today and the role that nuclear physics plays in many of them. In particular it is noted that the constraints on  $\Omega_{\text{baryon}}$  from big bang nucleosynthesis do not overlap with the constraints on  $\Omega_{\text{vis}}$  nor have significant overlap with the lower bound on  $\Omega$  from cluster studies. The former implies that the bulk of the baryons are dark and the latter is the principle argument for non-baryonic dark matter. A comparison with hot x-ray emitting gas in clusters is also made. The lower bound on the age of the universe from globular cluster ages (hydrogen burning in low mass stars) and from nucleocosmochronology also illustrates the Hubble constant requirement  $H_0 \leq 66 \text{ km/sec/Mpc}$  for  $\Omega_0 = 1$ . It is also noted that high values of  $H_0$  ( $\sim 80 \text{ km/sec/Mpc}$ ) even more strongly require the presence of non-baryonic dark matter. The lower limit on  $H_0$  ( $\geq 38 \text{ km/sec/Mpc}$ ) from carbon detonation driven type Ia supernova constrains long ages and only marginally allows  $\Omega_{\text{baryon}}$  to overlap with  $\Omega_{\text{cluster}}$ . Diagrams of  $H_0$ - $\Omega$  for  $\Lambda_0 = 0$  and  $\Lambda_0 \neq 0$  are presented to show that the need for non-baryonic dark matter is independent of  $\Lambda$ .

### 1. INTRODUCTION

In 1974, Gott, Gunn, Schramm and Tinsley<sup>1</sup> (hereafter, GGST) showed that a plot of the Hubble constant,  $H_0$ , versus the the dimensionless density parameter,

$$\Omega = \frac{\rho}{\rho_{\text{crit}}}, \quad (1)$$

where  $\rho$  is the mass density and

$$\rho_{\text{crit}} = \frac{3H_0^2}{8\pi G} \quad (2)$$

is the critical cosmological density, well illustrated the issues in physical cosmology, particularly for models with cosmological constant  $\Lambda = 0$ . Twenty years later we again use the  $H_0$ - $\Omega$  diagram and show that the constraints of GGST have not changed significantly, but the interpretation now illustrates the critical issues in physical cosmology today, namely the dark matter and age problems. As nuclear/particle astrophysicists we note with pride (or fear) how many of the most significant lines on the  $H_0$ - $\Omega$  diagram have their origin in nuclear physics arguments.

It will be shown how the  $H_0$ - $\Omega$  diagram dramatically illustrates that there are at least two dark matter problems, namely the bulk of the baryons are dark and the bulk of the matter in the universe is non-baryonic. It will also be shown that these two dark matter problems persist regardless of the value of  $H_0$ . These arguments center on the big bang nucleosynthesis (BBN) constraints on  $\Omega$  in baryons,<sup>2</sup>  $\Omega_{\text{baryon}}$ . We will also review the age constraints from globular cluster ages<sup>3</sup> and from nucleocosmochronology.<sup>4</sup> We will show with the  $H_0$ - $\Omega$  diagram that  $\Omega_0 = 1$  and the cosmological constant  $\Lambda_0 = 0$  requires  $H_0 \leq 66 \text{ km/sec/Mpc}$ . Variations in age- $H_0$ - $\Omega$  relationships for non-zero  $\Lambda$  are also discussed. A lower bound on  $H_0 \geq 38 \text{ km/sec/Mpc}$  from carbon-detonation powered type Ia supernova<sup>5</sup> is also plotted. For comparison, the information on the baryon content of hot x-ray emitting gas in clusters based on ROSAT measurements<sup>6</sup> is also discussed. This paper will now go through each of the constraints in turn and generate appropriate  $H_0$ - $\Omega$  diagrams.

## 2. COSMOLOGICAL MODEL

The Friedmann–Robertson–Walker (FRW) cosmological model provides a simple physical and mathematical model for describing the large scale structure of the universe by assuming the universe is isotropic and homogeneous. The smoothness of the background radiation is striking confirmation that the universe is isotropic at a level of 1 part in  $10^5$  (COBE). The assumption of homogeneity is less

straightforward to confirm; however, measurements of peculiar velocities of galaxies on very large scales<sup>7</sup> as well as radio source count studies<sup>8</sup> seem to indicate that it is valid. Within the FRW model the distance and time scales can be related to the Hubble constant,

$$H_0 = \frac{\dot{R}(t_0)}{R(t_0)}, \quad (3)$$

where  $R(t)$  is the scale factor of the universe and  $t_0$  is the present age. As we shall see, the value of the Hubble constant is still quite uncertain. Thus, in practice it is useful to introduce a dimensionless factor

$$h = \frac{H_0}{100 \text{ km/sec/Mpc}} \quad (4)$$

to express this uncertainty. The geometry of the universe is encoded in  $\Omega$  (and  $\Lambda$ ); for  $\Omega < 1$  ( $\Omega > 1$ ) and  $\Lambda = 0$  the universe is open and hyperbolic (closed and spherical), and for  $\Omega = 1$  it is open and flat. For the most part we shall assume the vacuum has no density nor pressure; in other words, we assume  $\Lambda = 0$  unless explicitly stated to the contrary.

In the FRW,  $\Lambda = 0$  model the present age of the universe is

$$t_0 = \frac{f(\Omega_0)}{H_0}, \quad (5)$$

where

$$f(\Omega_0) = \begin{cases} \frac{\Omega_0}{2(\Omega_0 - 1)^{3/2}} \left[ \cos^{-1}(2/\Omega_0 - 1) - \frac{2}{\Omega_0} \sqrt{\Omega_0 - 1} \right], & \Omega_0 > 1 \\ \frac{2}{3}, & \Omega_0 = 1 \\ \frac{\Omega_0}{2(1 - \Omega_0)^{3/2}} \left[ \frac{2}{\Omega_0} \sqrt{1 - \Omega_0} - \cosh^{-1}(2/\Omega_0 - 1) \right], & \Omega_0 < 1 \end{cases} \quad (6)$$

and  $\Omega_0$  is the present value of  $\Omega$

### 3. THE AGE OF THE UNIVERSE

The most stringent limits on the age of the universe come from the age of globular clusters and nucleocosmochronology. The age of globular clusters is essentially determined by the rate of hydrogen burning in low mass, metal poor stars. When the core of the star has been completely converted to helium, the star changes its structure and no longer lies on the main sequence of a Hertzsprung–Russel luminosity–temperature plot. The main sequence turnoff age is dependent on numerous aspects of the globular clusters, such as metallicity, helium diffusion in the stars, and the initial helium abundance.<sup>3</sup> While many groups have calculated globular cluster ages in the 14–16 Gyr range,<sup>9</sup> Shi<sup>10</sup> has shown that reasonable systematic assumptions in the calculations could lower the ages to  $12 \pm 2$  with a firm lower bound of  $t_0 \geq 10$  Gyr. This is also consistent with an independent study by Chaboyer.<sup>11</sup> This lower bound can be obtained trivially by noting that globular clusters should be burning hydrogen less rapidly than the sun since they have lower metallicity and a slightly lower mass. Our sun will exhaust the hydrogen in its core in about 10 Gyr (based on the hydrogen burning rate verified by the calibrated GALLEX experiment<sup>12</sup>). Thus globular clusters must have a lower bound on their age of  $t_0 \geq 10$  Gyr as quoted above.

Nucleocosmochronology provides information about time scales over which the elements in the solar system were formed. This method couples knowledge of present day abundance ratios, production ratios, and lifetimes of long-lived radioactive nuclides. The standard methods of determining nucleochronometric ages rely heavily on the adopted galactic evolution model. This can lead to large errors in the deduced galactic age. An alternative approach is to employ less restrictive, model-independent nucleocosmochronology which studies the constraints that can be made without specific reference to galactic nucleosynthesis models. When using radioactive decay alone, only a strict lower bound is possible.<sup>13</sup> In particular the mean age of the longest-lived chronometer,\*  $^{232}\text{Th}$  relative to  $^{238}\text{U}$ .

---

\*Although  $^{187}\text{Re}$  is longer lived in its ground state, its lifetime is dependent on its thermal environment, so is not useful for a lower bound. It does, however, constrain the maximum mean age (Ref. 14).

can be used to give an extremely conservative lower bound<sup>4,15</sup> of  $\sim 8$  Gyr. Since this bound assumes all nucleosynthesis occurs in a single event, it is obviously too extreme. We know that  $^{235}\text{U}$ ,  $^{244}\text{Pu}$ , and  $^{129}\text{I}$  all existed in measurable abundances when the solar system formed 4.6 Gyr ago, and free decay from a single production event several Gyr earlier would not be consistent (for example,  $^{129}\text{I}$  has a half-life of only 17 Myr and  $^{244}\text{Pu}$  only 82 Myr). Thus we know the production was more spread out than a single event. Meyer and Schramm<sup>4</sup> quantified this spreading out to show that the lower bound from chronology was  $\geq 9$  Gyr, and subsequent analysis by Schramm<sup>15</sup> using improved limits on the production ratios pushed the bound up to  $t_{\text{NC}} \geq 9.7$  Gyr.

The results from globular cluster and nucleocosmochronology provide a consistent lower bound for the age of the universe. We note that globular cluster ages and nucleocosmochronology do not provide a strong upper bound to the age of the universe since one could in principle add several Gyr of formation time to any such age determination. The lower bound does not have these problems since the extreme limit is globular cluster formation on a Kelvin–Helmholtz collapse time scale,  $t \sim 10^7$  yr at recombination,  $t \sim 10^5$  yr which yields formation times  $\ll 1$  Gyr after the big bang. It is not possible to form globular clusters earlier than this time. Based on the above results the age of the universe is constrained to be

$$t_0 \geq 10 \text{ Gyr.} \quad (7)$$

The resulting excluded region in the  $H_0$ – $\Omega$  plane is shown in Fig. 1 for  $\Lambda = 0$ , Fig. 2 for  $\Omega_\Lambda = 0.4$ , and Fig. 3 for  $\Omega_\Lambda = 0.8$ . Here  $\Omega_\Lambda$  is defined as above (1) with  $\rho_\Lambda = \Lambda/8\pi G$ .

#### 4. BIG BANG NUCLEOSYNTHESIS LIMITS

Standard homogeneous BBN accurately predicts the primordial abundances of the light elements over nine orders of magnitude in terms of a single parameter, the density of baryons,  $\rho_{\text{baryon}}$ . For the constraints on  $\Omega_{\text{baryon}}$  we adopt the recent determination by Copi, Schramm and Turner,<sup>2</sup>

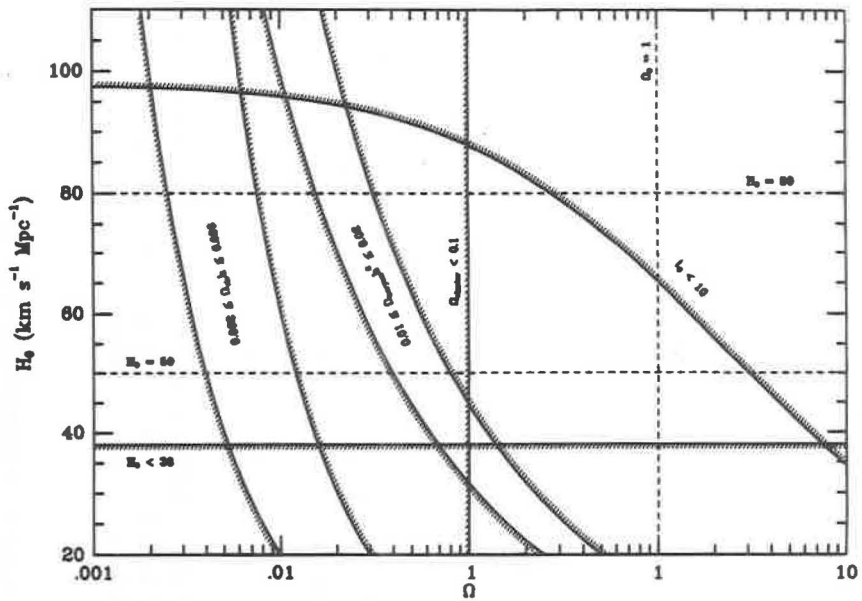


FIGURE 1 The  $H_0$ - $\Omega$  plane showing allowed and excluded regions. Shown here are the limits based on the age of the universe,  $t_0$ , the fraction of visible matter in the universe,  $\Omega_{\text{vis}}$ , the fraction of baryons in the universe,  $\Omega_{\text{baryon}}$ , the fraction of matter in clusters of galaxies,  $\Omega_{\text{cluster}}$ , and type Ia supernovae,  $H_0 \geq 38 \text{ km/sec/Mpc}$ . Also shown as dotted lines are the two current values for the Hubble constant,  $H_0 = 50 \text{ km/sec/Mpc}$  and  $H_0 = 80 \text{ km/sec/Mpc}$ , and the theoretically preferred  $\Omega_0 = 1$ . In this figure  $\Lambda = 0$ .

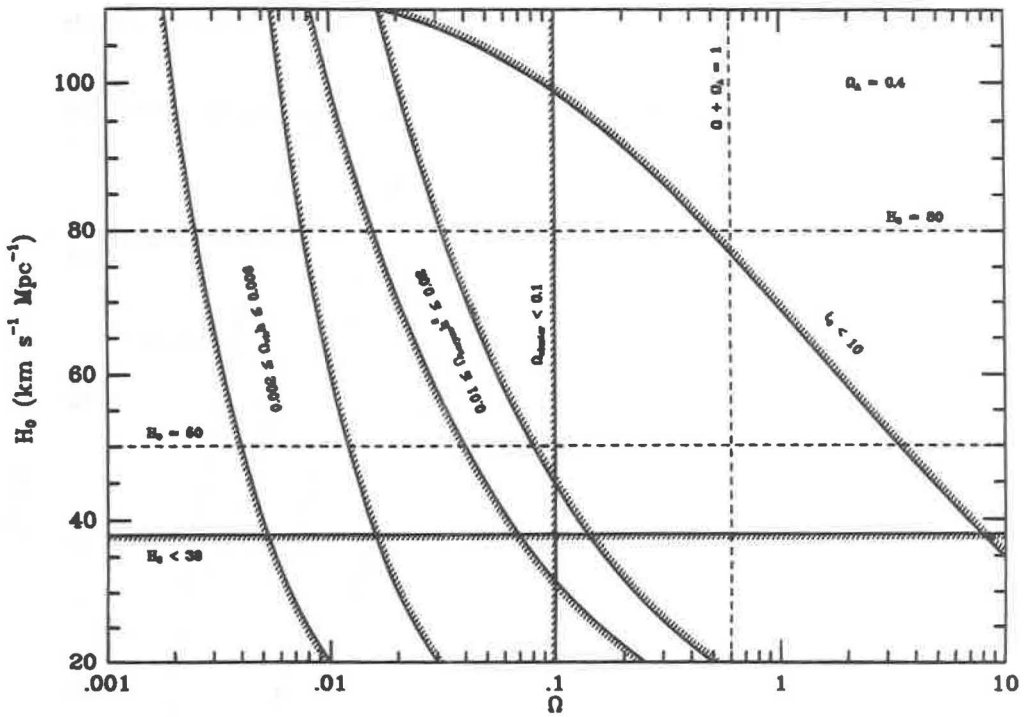


FIGURE 2 The  $H_0$ - $\Omega$  plane showing allowed and excluded regions as in Fig. 1 but with  $\Omega_\Lambda = 0.4$ .

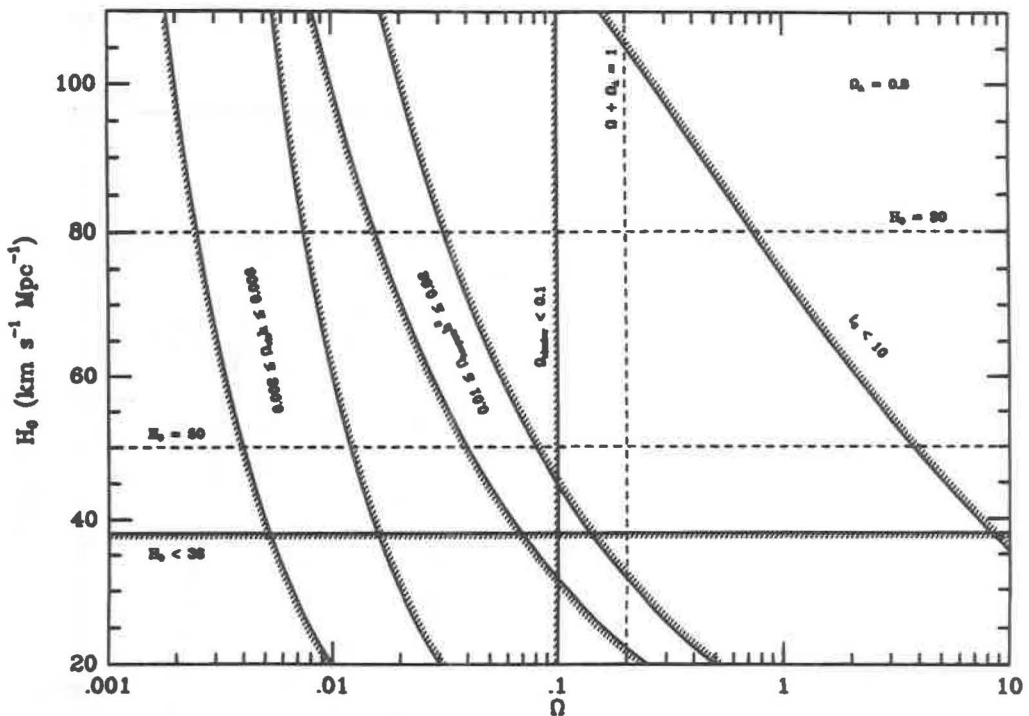


FIGURE 3 The  $H_0$ - $\Omega$  plane showing allowed and excluded regions as in Fig. 1 but with  $\Omega_\Lambda = 0.8$ .

$$0.01 \leq \Omega_{\text{baryon}} h^2 \leq 0.02. \quad (8)$$

Note that  $\rho_{\text{baryon}}$  is independent of the Hubble constant; thus the Hubble constant enters into  $\Omega_{\text{baryon}}$  only through  $\rho_{\text{crit}}$ . The curves defined by this choice and the excluded regions are shown in Fig. 1. Attempts to bypass these constraints with inhomogeneous models have been shown to fail in that the constraints on the light element abundances yield essentially the same constraints on  $\Omega_{\text{baryon}}$ .<sup>16</sup> Recently Tytler and Fann<sup>17</sup> have observed deuterium in a quasar absorption system that, if confirmed, restricts the baryon density to an extremely tight range near our quoted upper limit.<sup>18</sup>

It might be noted that one significant difference between our  $H_0$ - $\Omega$  diagram and that of GGST is that in 1974 BBN only provided an upper bound to  $\rho_{\text{baryon}}$  from deuterium,<sup>19</sup> whereas now we also have a lower bound on  $\rho_{\text{baryon}}$  from  $^3\text{He}$  plus deuterium arguments and we have the strict lithium constraints adding consistency to the picture.

## 5. DIRECT MEASUREMENTS OF $\Omega$

### 5.1. Visible Matter

The most straightforward method of estimating  $\Omega$  is to measure the luminosity of stars in galaxies and estimate the mass to light ratio,  $M/L$ , in a particular wave band. The mass density of visible objects is then given by

$$\rho_{\text{vis}} = \frac{M}{L} \mathcal{L}. \quad (9)$$

For example, for blue light  $\mathcal{L} = (1.6 \pm 0.2)h \times 10^8 L_{\odot} \text{ Mpc}^{-3}$  is the average luminosity density,<sup>20</sup> and for our Galaxy<sup>21</sup>

$$\frac{M}{L} = (6 \pm 3) \frac{M_{\odot}}{L_{\odot}}. \quad (10)$$

Here  $M_{\odot}$  is the mass of the sun and  $L_{\odot}$  is the luminosity of the sun. An alternative method of determining  $\Omega_{\text{vis}}$  employed by GGST

is to measure  $\mathcal{L}$  and  $M/L$  for the visible part of many different types of galaxies. This method relies on dynamical observations to determine  $M/L$  and produces  $\Omega_{\text{vis}}$  independent of  $H_0$ . Recent work following this method has produced values in excellent agreement with the value for our Galaxy.<sup>22,23</sup> The combination of these two methods produces a range consistent with

$$0.002 \leq \Omega_{\text{vis}} h \leq 0.006. \quad (11)$$

The curves defined by this range and the excluded regions are shown in Fig. 1.

## 5.2. Dynamical Measurements

Numerous methods for dynamically measuring the density of the universe have been developed, all of which give complimentary results. A review of many of these methods can be found in Ref. 22. We shall highlight a few of these methods.

The simplest means of measuring mass inside a radius,  $r$ , is via Kepler's third law,

$$GM(r) \approx v^2 r. \quad (12)$$

If the mass were solely associated with the light, then we would expect  $v \propto r^{-1/2}$  for some object outside of the core of the galaxy. Instead it is observed that  $v \approx \text{constant}$  for objects far from the center of the galaxy. This indicates that dark matter exists in a halo around the galaxy. Typical estimates of the mass in halos from this method give  $\Omega_{\text{halo}} \approx 0.05$ . This dark matter could in principle be dark baryons; however, see the discussion on MACHOS below. Note that estimates of the mass density from dynamics scale with  $h^2$  as does  $\rho_{\text{crit}}$ ; thus  $\Omega$  is independent of  $H_0$ .

Measurements of average velocity dispersion and average separation of galaxies in clusters provide a means of assessing the amount of matter associated with clusters. It is generally observed that the velocity of galaxies approaches a constant value for large distances from the cluster core. As noted above, this indicates the presence of significantly more mass than is visible in the galaxies themselves. A detailed statistical analysis of galaxy dynamics<sup>24</sup> yields

$$\Omega_{\text{cluster}} = 0.15 \pm 0.06. \quad (13)$$

An independent method of verifying this value of  $\Omega_{\text{cluster}}$  is due to the observation of giant luminous arcs by Lynds and Petrosian.<sup>25</sup> These arcs are the image of a bright background object that falls in the line of sight of a cluster core. The mass of the cluster serves as a gravitational lens of this background object, producing the arc.<sup>26</sup> Although the modeling of the mass distribution in the cluster can be quite complex, the general prediction of  $\Omega_{\text{cluster}} \sim 0.2$  is in good agreement with the above value.

Finally we note that many of these methods can be applied on even larger scales. For example, the peculiar velocities of clusters of galaxies can be studied similarly to what has been done for galaxies.<sup>7</sup> The result of these types of studies is a consistent bound of  $\Omega > 0.3$ . To be conservative we shall adopt

$$\Omega_{\text{cluster}} > 0.1. \quad (14)$$

This limit is shown in Fig. 1.

### 5.3. Baryon Content of Clusters

In addition to providing a measure of  $\Omega$ , clusters also provide a means of estimating  $\Omega_{\text{baryon}}$ . The three main mass components of clusters of galaxies are stars in galaxies, hot intracluster gas, and dark matter. The first two are comprised solely of baryons. Optical observations provide an estimate of the baryon mass in stars, and x-ray studies provide an estimate of the baryons in hot gas. These two quantities together provide an estimate of the total baryon mass in the cluster. The total mass of the cluster is more difficult to determine. It is sensitive to numerous assumptions. In particular the cluster is typically assumed to be spherical and in dynamical equilibrium (virialized). If either of these assumptions is not valid the derived total mass could be incorrect. Frequently structure formation models are employed to remove some of this sensitivity. White, Navarro, Evrard and Frenk<sup>6</sup> employed a “standard” cold dark matter (CDM) model ( $\Omega_0 = 1$ ) coupled with optical and x-ray studies to deduce a baryon fraction for the Coma cluster of

$$\Omega_{B,C} = (0.009 \pm 0.002) + (0.05 \pm 0.01)h^{-3/2}. \quad (15)$$

Here the first term is due to baryons in stars and the second to baryons in hot gas. Note that  $\Omega_{B,C}$  is defined by

$$\Omega_{B,C} = \frac{M_{\text{baryon}}}{M_{\text{tot}}}, \quad (16)$$

where  $M_{\text{baryon}}$  is the mass in baryons of the cluster and  $M_{\text{tot}}$  is its total mass. The region defined by these limits is shown in Fig. 4.

If clusters are a fair sample of the universe, then we expect  $\Omega_{\text{baryon}} = \Omega_{B,C}/\Omega_0$ , which is clearly not the case if  $\Omega_0 = 1$ . The question of whether galaxies in clusters trace the dark matter is still an open one. Babul and Katz<sup>27</sup> found that baryons in an  $\Omega_0 = 1$  CDM model are more strongly concentrated than the dark matter. Thus  $\Omega_{B,C} > \Omega_{\text{baryon}}$ , and there is no inconsistency in the results. Alternate models with some admixture of hot dark matter also yield  $\Omega_{B,C} > \Omega_{\text{baryon}}$ . At present there are still a number of difficulties to be worked out in the interpretation of the x-ray gas in clusters result. It is clear, however, that this observation provides important constraints on cluster formation models.

#### 5.4. $\Omega_0 = 1$ ?

A well-known feature of FRW cosmologies is at an epoch  $t$ , if  $\Omega < 1$  ( $\Omega > 1$ ), the universe evolves towards  $\Omega = 0$  ( $\Omega = \infty$ ) on a time scale  $\sim 1/H(t)$  (see Ref. 28). Notice that  $\Omega = 1$  is an unstable equilibrium point. At early times  $R(t)$  was changing rapidly and  $H(t)$  was large. Thus all evolutionary changes occurred on much shorter time scales. Since the universe is clearly not more than an order of magnitude away from  $\Omega = 1$  today, it must have been unity to high accuracy in all earlier epochs. In particular we have a good understanding of the physics of the universe at the beginning of BBN ( $t \sim 1$  sec). If we trace  $\Omega$  to the epoch of BBN, we find that  $\Omega$  must have been unity to  $\sim 17$  decimal places at that time. The extreme amount of tuning required to satisfy this is an initial condition within the standard big bang model.

The theory of inflation succinctly explains this fine tuning, the homogeneity and isotropy of the universe, and other initial conditions

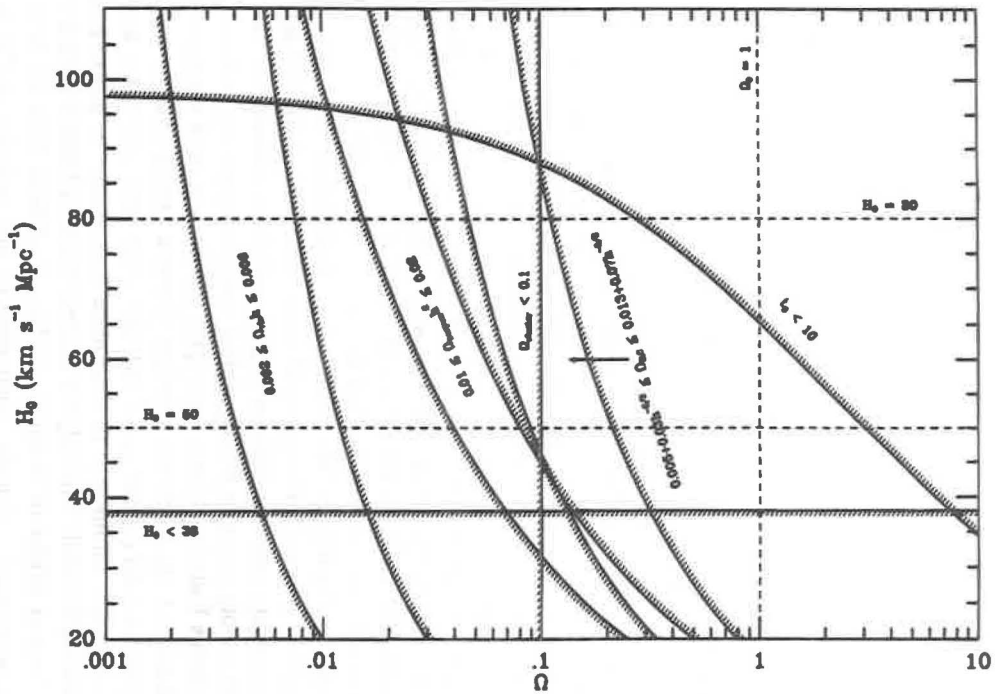


FIGURE 4 The  $H_0$ - $\Omega$  plane showing allowed and excluded regions as in Fig. 1 but with the addition of the limits from baryons in clusters,  $\Omega_{\text{B},\text{C}}$ .

with physics motivated by particle physics theory. Most models of inflation require the universe to be perfectly flat,  $\Omega_0 = 1$ , or at least  $\Omega_{\text{matter}} + \Omega_{\Lambda} = 1$ . Though this is not a measurement and is an untested theory, it provides a compelling theoretical argument for  $\Omega_0 = 1$ . Furthermore, recent measurements on the largest scales<sup>7</sup> indicate that  $\Omega_0 \approx 1$ . Though there is no firm evidence, we show our bias towards  $\Omega_0 = 1$  by plotting this value as a dashed line in Figs. 1 and 4 and the line  $\Omega_{\text{matter}} + \Omega_{\Lambda} = 1$  in Figs. 2 and 3.

## 6. MEASUREMENTS OF $H_0$

The observational determination of  $H_0$  has a long and interesting history beginning with the original measurement by Hubble<sup>29</sup> of  $H_0 = 550$  km/sec/Mpc. Since this time the value has been reduced by about a factor of  $\sim 10$  due to a number of systematic errors in the assumptions used by Hubble. Currently the measurements fall into two distinct groups:  $H_0 \approx 80$  km/sec/Mpc (see Ref. 30) and  $H_0 \approx 50$  km/sec/Mpc (see Ref. 31). These two values are represented by dashed lines in Fig. 1. At present possible systematic errors do allow for a consistent resolution of the two values at  $H_0 \sim 66$  km/sec/Mpc which happens to also be near the value recently obtained by Riess, Press and Kirshner.<sup>32</sup> Notice from Fig. 2 that  $H_0 \sim 80$  km/sec/Mpc can be made consistent with a flat universe if  $\Omega_{\Lambda} \sim 0.4$ .

The main difficulty in determining  $H_0$  is establishing the distance to an object. Although it is relatively easy to establish the redshift of an object, its absolute distance is quite difficult to determine. The redshifts for objects observed by Hubble are the same today, whereas the distances Hubble estimated are quite far from present estimates. The traditional approach for absolute distance measurements is to identify a standard candle (an object with a known luminosity) and use its apparent luminosity to determine a distance. In practice a given standard candle can only be observed over a limited distance range. Thus a ladder of distances to known objects must be built starting with nearby objects. Each rung on the distance ladder is governed by a different standard candle. Slight errors or disagreements on an early rung can correspond to large uncertainties and differences for very distant objects and thus different values for the Hubble constant.

One method of minimizing this problem is to use type Ia supernovae where the luminosities are known, at least roughly, from the physics and they can be observed over a large range of distances. Detailed calibrations of type Ia supernovae involve establishing distances by other techniques, including Cepheid variable stars from the Hubble space telescope, to nearby galaxies where such supernovae have exploded. This method tends to give a value of  $H_0 \sim 50$  km/sec/Mpc. Note that this technique can also be used to bound  $H_0$  from below. The extreme lower bound comes from the fact that type Ia supernovae seem to be caused by a C–O white dwarf star burning its C–O to Fe via carbon detonation/deflagration. Assuming that the entire  $1.4M_\odot$  Chandrasekhar mass of the white dwarf is pure carbon and is completely converted to iron provides the maximal energy release and the limit<sup>5</sup>

$$H_0 \geq 38 \text{ km/sec/Mpc.} \quad (17)$$

We show this lower limit in Fig. 1.

## 7. TWO DARK MATTER PROBLEMS

The so-called two dark matter problems are (i) most of the baryons in the universe are dark (baryonic dark matter) and (ii) most of the matter in the universe is non-baryonic (non-baryonic dark matter). Both of the problems are illustrated in Fig. 1. Note that regardless of the value of  $H_0$ ,  $\Omega_{\text{vis}}$  does not intercept  $\Omega_{\text{baryon}}$ . Similarly, on the high  $\Omega$  side,  $\Omega_{\text{baryon}}$  only marginally intersects  $\Omega_{\text{cluster}}$  at very low  $H_0$  values. Thus, except for  $H_0 < 50$  km/sec/Mpc, we already know that  $\Omega_{\text{cluster}}$  requires non-baryonic dark matter. High values of  $H_0$  amplify the need for non-baryonic dark matter.

### 7.1. Baryonic Dark Matter

From Fig. 1 we see that the regions defined by  $\Omega_{\text{vis}}$  and  $\Omega_{\text{baryon}}$  do not overlap for any value of  $H_0$  shown. Thus, even if all of the visible matter is baryonic, most (at least 70%) of all baryons must be dark. Although the halo of our galaxy could be composed of dark baryonic objects such as brown dwarfs and Jupiters, known as massive com-

pact halo objects (MACHOS), Gates, Gyuk and Turner,<sup>33</sup> using the relative paucity of microlensing events in the direction of the Large Magellanic Cloud and the high number of such events towards the galactic bulge, have argued that less than 40% of the halo can be MACHOS, indicating that the halo probably also includes a non-baryonic component. This latter point seems to require that at least some of the non-baryonic dark matter must be cold so it can condense in halos. One loophole to this is black holes with  $M \sim 10^3 M_\odot$ , too small to tidally disrupt star clusters and yet big enough to avoid overproduction of heavy elements.

## 7.2. Non-Baryonic Dark Matter

As noted above, if  $H_0 \geq 50$  km/sec/Mpc, the measurement of  $\Omega_{\text{cluster}}$  already requires non-baryonic dark matter. Moreover, the observational evidence suggesting  $\Omega_0 \approx 1$  and the theoretical arguments of avoiding fine tuning (such as from inflation) requiring a flat universe further strengthens this requirement. In the case of  $\Omega_0 \approx 1$  non-baryonic dark matter is required for all values of  $H_0$  since  $\Omega_{\text{baryon}} < 1$  for any value of  $H_0$ . Notice that even for  $\Lambda_0 = 0.8$  (Fig. 3) the baryonic and non-baryonic dark matter arguments are unchanged.

## 8. SUMMARY

We have used the  $H_0$ - $\Omega$  diagram to illustrate the nature of key problems in physical cosmology and the role nuclear physics plays in them. We have seen how BBN serves to define the two dark matter problems. We have seen that if  $H_0 > 50$  km/sec/Mpc, then  $\Omega_{\text{cluster}} > \Omega_{\text{baryon}}$ , requiring the existence of non-baryonic dark matter. If  $\Omega_0 = 1$  as current observational and theoretical work indicates, then non-baryonic dark matter is required for all values of  $H_0$ . Finally we have reviewed the age constraints from globular clusters and nucleocosmochronology to show that  $\Lambda_0 = 0$  requires  $H_0 \leq 66$  km/sec/Mpc.

### Acknowledgments

We would like to acknowledge our previous collaborators D. N. Dearborn, J. R. Gott, J. E. Gunn, B. S. Meyer, K. A. Olive, P. J. E. Peebles, G. Steigman, M. S.

Turner, X. Shi, J. W. Truran, and G. J. Wasserburg whose work we have drawn upon. We also gratefully remember Beatrice Tinsley who was the person who brought the GGST collaboration together. This work has been supported in part by NSF grant AST 90-22629, DOE grant DE-FG02-91-ER40606, and NASA grant NAG5-2788 and by a NASA GSRP fellowship.

**CRAIG J. COPI**

*Department of Physics,  
The University of Chicago,  
Chicago, Illinois 60637-1433*

*and*

*NASA/Fermilab Astrophysics Center,  
Fermi National Accelerator Laboratory,  
Batavia, Illinois 60510-0500*

**DAVID N. SCHRAMM**

*Department of Physics,  
The University of Chicago,  
Chicago, Illinois 60637-1433*

*and*

*NASA/Fermilab Astrophysics Center,  
Fermi National Accelerator Laboratory,  
Batavia, Illinois 60510-0500*

*and*

*Department of Astronomy and Astrophysics,  
Enrico Fermi Institute,  
The University of Chicago,  
Chicago, Illinois 60637-1433*

## References

1. J. R. Gott, J. E. Gunn, D. N. Schramm and B. M. Tinsley, *Astrophys. J.* **194**, 543 (1974).
2. C. J. Copi, D. N. Schramm and M. S. Turner, *Science* **267**, 192 (1995).
3. X. Shi, D. N. Schramm, D. S. P. Dearborn and J. W. Truran, *Comments Astrophys.* (1995, in press).
4. B. S. Meyer and D. N. Schramm, *Astrophys. J.* **311**, 406 (1986).
5. W. D. Arnett, D. Branch and J. C. Wheeler, *Nature* **314**, 337 (1985).
6. S. D. M. White, J. F. Navarro, A. E. Evrard and C. S. Frenk, *Nature* **366**, 429 (1993).
7. A. Dekel, *Ann. Rev. Astron. Astrophys.* **32**, 371 (1994); also see M. Davis, UC Berkeley preprint (1995).
8. P. J. E. Peebles, D. N. Schramm, E. L. Turner and R. G. Kron, *Nature* **352**, 769 (1991).
9. D. A. VandenBerg, *Astrophys. J.* **391**, 685 (1992); P. A. Bergbusch and D. A. VandenBerg, *Astrophys. J. (Suppl.)* **81**, 163 (1992); A. Sandage, *Astron. J.* **106**, 719 (1993).
10. X. Shi, *Astrophys. J.* (1995, in press).
11. B. Chaboyer, *Astrophys. J. Lett.* (1995, in press).

12. P. Anselmann *et al.* (GALLEX collaboration), *Phys. Lett. B* **342**, 440 (1995).
13. D. N. Schramm and G. J. Wasserburg, *Astrophys. J.* **162**, 57 (1970).
14. B. S. Meyer *et al.*, in *Recent Advances in the Study of Nuclei Away from Stability*, eds. R. Meyer and D. Brenner (American Chemical Society Press, Washington, DC, 1985).
15. D. N. Schramm, in *Astrophysical Ages and Dating Methods*, eds. E. Vangioni-Flam *et al.* (Editions Frontières, Gif-sur-Yvette, France, 1990), pp. 365–383.
16. D. Thomas *et al.*, *Astrophys. J.* **406**, 569 (1993); K. Jedamzik, G. M. Fuller, G. J. Mathews and T. Kajino, *Astrophys. J.* **442**, 423 (1994).
17. D. Tytler and R. Fann, presented at the ESO symposium on Lyman- $\alpha$  clouds, Munich (1994).
18. D. N. Schramm and C. J. Copi, in *Proc. of Cosmion-94*, Moscow, Dec. 4–14, 1994 (Editions Frontières, Gif-sur-Yvette, France, 1995, in press).
19. H. Reeves, J. Audouze, W. A. Fowler and D. N. Schramm, *Astrophys. J.* **179**, 909 (1973).
20. B. Binggeli, A. Sandage and G. A. Tammann, *Ann. Rev. Astron. Astrophys.* **26**, 509 (1988).
21. S. M. Faber and J. S. Gallagher, *Ann. Rev. Astron. Astrophys.* **17**, 135 (1979).
22. P. J. E. Peebles, *Principles of Physical Cosmology* (Princeton University Press, Princeton, 1993).
23. M. Persic and P. Salucci, *Mon. Not. Roy. Astron. Soc.* **258**, 14 (1992).
24. M. Davis and P. J. E. Peebles, *Astrophys. J.* **267**, 465 (1983).
25. R. Lynds and V. Petrosian, *Bull. Amer. Astron. Soc.* **18**, 1014 (1986).
26. B. Paczyński, *Nature* **325**, 572 (1987).
27. A. Babul and N. Katz, *Astrophys. J.* **406**, L51 (1993).
28. R. H. Dicke, *Gravitation and the Universe* (American Philosophical Society, Philadelphia, 1970); S. Chandrasekhar in private communication has noted to us that Eddington, Lemaître, and Robertson were all aware of this argument in the 1930's, but  $\Lambda = 0$  cosmologies were viewed as inconsistent with observations since at the time  $H_0 \sim 500$  km/sec/Mpc.
29. E. Hubble, *Proc. Nat. Acad. Sci.* **15**, 168 (1929).
30. M. J. Pierce *et al.*, *Nature* **371**, 385 (1994); W. L. Freedman *et al.*, *ibid.*, 757 (1994).
31. A. Sandage *et al.*, *Astrophys. J.* **423**, L13 (1994).
32. A. Riess, W. H. Press and R. Kirshner, *Astrophys. J.* **438**, L17 (1995).
33. E. Gates, G. Gyuk and M. S. Turner, *Phys. Rev. Lett.* (1995, in press); also see C. Alcock *et al.* (MACHO collaboration), *Phys. Rev. Lett.* (1995, in press).